Data Processing and Analysis of Performance Measurements from Ingenuity Rotors in the Jet Propulsion Laboratory 25-ft Space Simulator

Natasha Schatzman
natasha.schatzman@nasa.gov
Aerospace Engineer
NASA Ames Research Center
Moffett Field, CA, USA

Athena Chan
athena.chan@nasa.gov
Mechanical Engineer
NASA Ames Research Center
Moffett Field, CA, USA

Vinod Gehlot
vinod.p.gehlot@jpl.nasa.gov
Robotics Systems Engineer
NASA Jet Propulsion Laboratory
California Institute of Technology,
Pasadena, CA, USA

Kenneth Glazebrook
kenneth.j.glazebrook@jpl.nasa.gov
Mechatronics Engineer
NASA Jet Propulsion Laboratory
California Institute of Technology,
Pasadena, CA, USA

ABSTRACT

The success of Ingenuity completing over 71 flights on Mars has resulted in the possible use of two further optimized Ingenuity-sized helicopters to retrieve samples for the planned Mars Sample Return campaign. Data to validate performance for several rotor speeds, densities, configurations, and collectives will aid in the design process and help in understanding Ingenuity's current performance limitations. Tests were performed at the Jet Propulsion Laboratory (JPL) in the 25-foot Space Simulator, which include the Engineering Design Model 1 (EDM-1) with and without a cruciform box, and the Transonic Rotor Test (TRT) which is a single rotor setup featuring the same blade geometry as EDM-1 but designed to spin at much higher RPMs. The experimental setup, test matrix, data processing, data quality, and the performance results for EDM1 and TRT campaigns are presented.

NOTATION

A	Rotor area (m^2)
C_P	Rotor power coefficient $\left(\frac{P}{\rho A(\Omega R)^3}\right)$
C_Q	Rotor torque coefficient $\left(\frac{Q}{\rho A(\Omega R)^2 R}\right)$
C_T	Rotor thrust coefficient $\left(\frac{T}{\rho A(\Omega R)^2}\right)$
C_T/σ	Rotor thrust coefficient over rotor solidity
c	Chord (m)
FM	Figure of merit $\left(\frac{C_T^{3/2}}{\sqrt{2}C_P}\right)$
M_{tip}	Rotor hover tip Mach number
N_b	Number of blades
P	Power (W)
$P_{electric}$	Electrical power (W)
Q	Shaft torque (N-m)
R	Rotor radius (m)
Re	Reynolds number
RPM	Rotor rotational speed $\left(\frac{rev}{min}\right)$
T	Thrust (N)
t	Time (seconds)
σ	Rotor solidity, $\left(\frac{N_b c}{\pi R}\right)$
$\overline{\sigma}$	Standard deviation
ρ	Air density $\left(\frac{kg}{m^3}\right)$
Ω	Rotational frequency

Presented at the VFS 6th Decennial Aeromechanics Specialists' Conference, Santa Clara, CA, USA Feb.6-8, 2024.

INTRODUCTION

Ingenuity arrived at Mars's Jezero Crater on February 18th, 2021 and became the first helicopter to fly on another planet. To date, Ingenuity has conducted over 68 successful flights, Fig. 1 shows Ingenuity after completing its 48th flight (Ref. 1). Ingenuity's success resulted in the possible use of two further optimized Ingenuity-sized helicopters to retrieve samples for the planned Mars Sample Return campaign (Ref. 2). The baseline concept for the two Sample Recovery Helicopters retains much of Ingenuity's design due to its proven performance, with the addition of a robotic arm to retrieve soil sample tubes, and wheels for surface mobility (Ref. 2).

To advance this effort, there is the need to validate aerodynamic performance of Ingenuity for several rotor speeds, atmospheric densities, configurations, and collectives to aid in the design process and help understand Ingenuity's current performance limitations.

Collaboration between JPL, NASA Ames, and AeroVironment enabled two rotor test campaigns to be conducted at the Jet Propulsion Laboratory (JPL) in the 25-foot Space Simulator to determine the performance limits of the heritage Ingenuity blades as part of SRH research (Ref. 3).

The first test was of the Engineering Design Model 1 (EDM-1), see Fig. 2. The EDM-1 is nearly identical to Ingenuity, except that the pitch links have been modified to allow for higher collective angles, up to ~23-degrees, to identify stall and power limits. The EDM-1 was also tested with a cruciform box intended to simulate the Lift-off Adapter and Inverted Retention (LAIR) shell, which is the

initial takeoff platform on Mars for the SRHs. The second test was the Transonic Rotor Test (TRT), a single rotor setup featuring the same blade geometry as EDM-1 but designed to spin at much higher RPMs; this test determined the RPM limit for compressibility effects. The experimental setup, test matrix, data processing, data quality, and the performance results for EDM-1 and TRT campaigns will be presented and discussed.

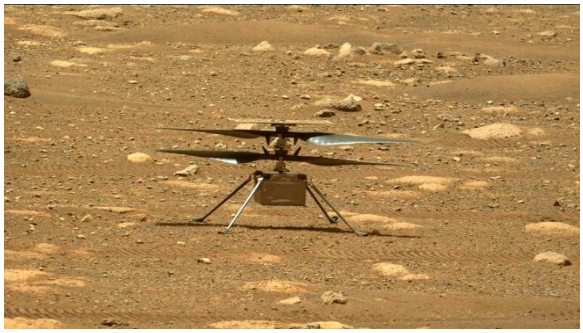

Figure 1. Ingenuity on surface of Mars after completing 67 flights.

Figure 2. EDM-1 Model test article.

TEST OVERVIEW

The purpose of the EDM-1 and TRT tests is to answer the central question, "How can we lift a heavier vehicle while maintaining as much of the heritage design from Ingenuity?" To answer this question, three primary methods of achieving such objectives were identified, which includes the following 1) increase angle of attack/collective, 2) increase RPM, and 3) increase rotor diameter. The EDM-1 and TRT tests explored option 1, increasing blade collective and option 2, spinning at higher RPMs. Primary objectives and a summary of EDM-1 without the cruciform box, EDM-1 with the cruciform box, and TRT are discussed.

EDM-1 without the cruciform box

The primary objective of EDM-1 without the cruciform box was to establish the performance limits of the heritage Ingenuity blades. In other words, the test campaign sought to drive the rotors into stall, determine usable thrust, and answer the question, "Can Ingenuity geometry support a 2.5 kg vehicle by flying closer to stall?". While changing the collective can increase lift, it can also increase the blade loading. Thus, collective can only be increased up until a certain point before the blade loading becomes so great that efficiency drops and/or even damages the blades.

EDM-1 without the cruciform box testing started on November 1, 2022 and ended on November 9, 2022. The first portion of this test (EDM-1-Test 1) was conducted at lower densities (~0.01 kg/m^3) in an effort to conserve power. The collective angle reached a maximum of 22.5-degrees. Single upper and lower rotor runs were used to gather the necessary data to generate a motor efficiency function.

The second portion of testing EDM-1 without the cruciform box (EDM-1-Test 2) began on February 15, 2023 and ended on March 8, 2023. This portion was, for the most part, conducted at a higher density of ~0.0185 kg/m^3. The final run in Test 2 took place at a density of ~ 0.03 kg/m^3. Test 2 tested collective angles up to 19.5-degrees. Single upper and lower rotor runs were also completed to characterize electromechanical drive system efficiency.

EDM-1 with the cruciform box

The primary objective of the EDM-1 with the cruciform box was to collect data on how the vehicle reacts when spinning up next near a structure that represents the mission's helicopter accommodation hardware (the LAIR). Test 3 attempted to mimic conditions the SRHs will experience when lifting off from the LAIR.

The EDM-1 with the cruciform box test took place from March 20, 2023, to March 22, 2023, with the primary goal of further investigating aero performance when spun at higher densities and collectives in the presence of a cruciform box. Runs included densities of ~0.01 kg/m^3, ~0.0185 kg/m^3, and ~0.03 kg/m^3, and had a maximum collective angle of 21.5-degrees.

TRT

The primary objectives of TRT were to test the Ingenuity single rotor at higher speeds, searching for signs of drag divergence.

The TRT runs started on January 17, 2023 and ended on January 18, 2023. The TRT setup only included a single rotor consisting of two Ingenuity blades (not a coaxial dual rotor design like Ingenuity/EDM-1). TRT was conducted at a density of ~0.01 kg/m^3 only.

EXPERIMENTAL SETUP

EDM-1 without the cruciform box, EDM-1 with the curariform box, and TRT were conducted in the JPL 25-ft Space Simulator as shown in Fig. 3 a) through c), respectively. For all tests, the simulator was evacuated of all air and then backfilled with CO_2 to the target density for the planned test. A Mechanical Ground Support Equipment (MGSE) gantry was used to support the test articles. A second independent MGSE structure was used to hold the cruciform box over EDM1 when needed. In all cases the rotor system(s) were mounted upside down relative to the chamber's floor to reduce ground effect caused by the downwash.

Instrumentation and Data Acquisition

Five acquisition systems were used to acquire data, including: helicopter control, force and torque (upper and lower rotor combined), accelerometers, microphone, and thermocouples. For performance analysis, only the helicopter control and force and torque data acquisition systems are utilized. EDM-1 used Keysight's BenchVue software in lieu of a traditional data acquisition system to record data from power supplies. TRT used AV's inhouse software for recording voltage, current, and power data. The EDM-1 and TRT test both used the same Ingenuity rotor geometry as shown in Fig. 4.

An ATI Industrial Automation Force/Torque Sensor (FTS) was mounted between the test article and the MGSE structure. The FTS collected rotor-generated force and torque data (for rotor performance) and is shown in Fig. 5. Additional sensors on the MGSE included multiple tri-axial accelerometers used to assess its dynamic behavior during operation at resonances. A microphone recorded the acoustic signature of each run, and several cameras provided visual monitoring to the team during each test. Thermocouples were used to measure chamber temperature for atmospheric density calculations, and to monitor hardware temperatures for safety. The 25-ft Space Simulator also has pressure transducers that contribute to the atmospheric density calculation.

a)

b)

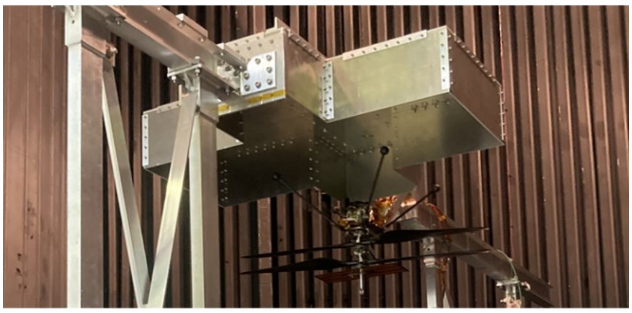

c)

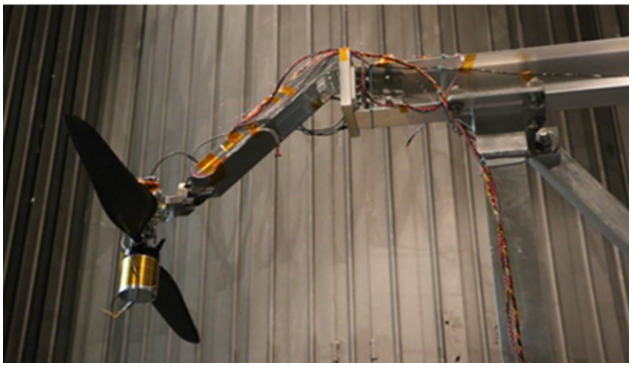

Figure 3. Test set up for a) EDM-1 without cruciform box, b) EDM-1 with cruciform box, and c) TRT.

Sampling rates for EDM-1 and TRT were as follows: force and torque (500 Hz), motor power(s) (250 Hz), control inputs and RPM (~500 Hz), and accelerometers (20 kHz). Data was acquired continuously for ~60 seconds for each run. Each run contained multiple flight conditions (i.e., changes in collective, cyclic, and RPM), which required data processing efforts to identify the start and stop of each test point.

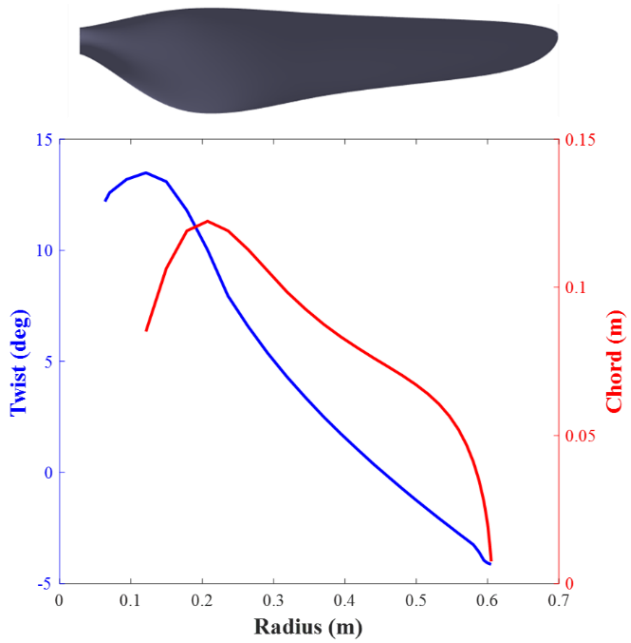

Figure 4. Ingenuity blade twist and chord along radius.

Figure 5. Force/Torque sensor used for the test campaigns

Flight Conditions and Test Matrix

The chamber conditions for the EDM-1 and TRT were set to mimic the densities found at Jezero Crater Rim with 1.5 m altitude. The SRH design assumption required density to be greater than 0.012 kg/m^3.

Flight conditions and configurations were chosen to determine the maximum lift that can be achieved using the heritage design from Ingenuity. Maximum lift was investigated during testing by increasing collective pitch angle and RPM.

Furthermore, performance of EMD-1 with and without the cruciform box were also investigated. A summary of test conditions for varying densities, Mach tip numbers, Reynolds numbers, and with and without the presence of the cruciform box is shown in Table 1 and Fig. 6.

Five distinctive types of data collecting runs were conducted: step, sweep, trim, doublet, and triangle. Only step runs are presented in this paper for both EDM-1 and TRT performance figures.

Step runs encompass multiple flight conditions within a single run. The collective is increased/decreased in set increments throughout the duration of the run. 2-3 seconds of dwell time occurs between each collective change. Step runs allows for collecting non-transient data for multiple flight conditions in one go.

Sweep runs increase/decrease collective at a constant rate throughout the duration of the run, allowing for transient flight data collection.

Trim runs involve actively controlling the rotor collective to hit a target thrust or power setting.

Doublet runs include the usage of cyclic. Both upper and lower rotors have their own set of cyclic control. During doublet runs, collective is maintained at a set degree, but the cyclic inputs are varied as step inputs.

Triangle runs involve rapidly increasing and decreasing the collective in short, back-to-back bursts. The collected data aids with understanding the rotor system response.

Checkout runs—such as battery health assessments, resonance searches, and the snapdragon sleep tests—are excluded from this paper. Explanation of the various types of run (e.g., step, trim, doublet, sweep, triangle) will be discussed in data processing section).

EDM-1: Test 1 without the cruciform box focused on conducting collective sweeps ranging from 1° to 22.5°. A handful of trim and doublet runs where $C_T/\sigma = 0.135$ and $C_T/\sigma = 0.17$ were conducted as well. For all runs, the chamber temperature ranged from 18.5 – 22.25 °C.

EDM-1: Test 2 consisted primarily of collective sweeps ranging from 1.5° to 19.5°. Many doublet runs were also completed with $C_T/\sigma = 0.135$, $C_T/\sigma = 0.15$, and $C_T/\sigma = 0.17$. The chamber temperature ranged from 19.62 – 22.47 °C.

Table 1. EDM-1 and TRT test matrix.

Test	Rotor	RPM	Density [kg/m^3]	M_{TIP}	Re
EDM-1 w/o cruciform box	Both	2200	0.0100	0.52	5254
	Upper	2200	0.0103	0.52	5367
	Lower	2200	0.0103	0.52	5404
	Both	2200	0.0141	0.52	7382
	Both	2043	0.0184	0.48	8971
	Upper	2043	0.0184	0.48	8895
	Lower	2043	0.0185	0.48	8986
	Both	2200	0.0186	0.52	9757
	Both	2550	0.0185	0.60	11230
	Upper	2550	0.0185	0.60	11249
	Lower	2550	0.0185	0.60	11249
	Both	2043	0.0300	0.48	14549
EDM-1 w/ cruciform box	Both	2200	0.0103	0.52	5396
	Both	2043	0.0185	0.48	8946
	Both	2043	0.0303	0.48	14674
TRT	Single	2740	0.0099	0.65	6461
	Single	2950	0.0099	0.70	6950
	Single	3160	0.0099	0.75	7437
	Single	3375	0.0099	0.80	7944
	Single	3585	0.0099	0.85	8452

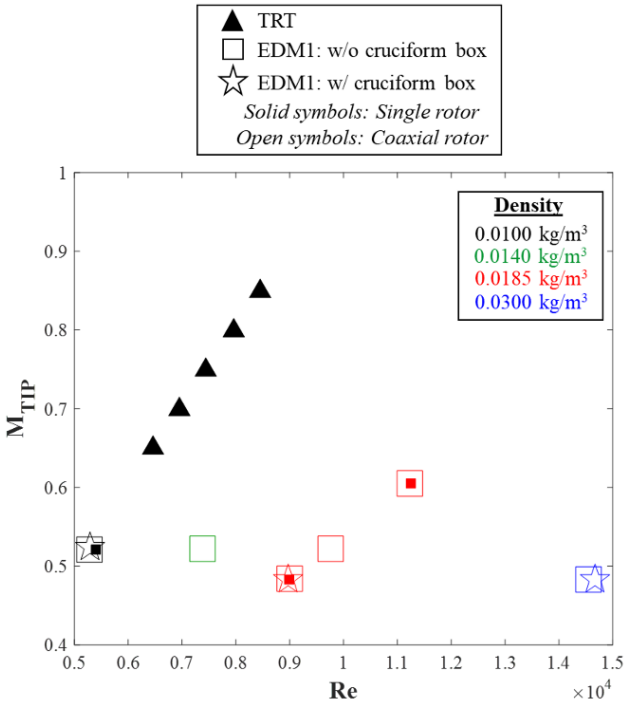

Figure 6. EDM-1 and TRT test conditions.

EDM-1: Test 3 with the cruciform box included a cruciform box placed below (aerodynamically below, in the rotor wake; physically above the inverted helicopter) the fuselage of the EDM1. Test 3 consisted of collective sweeps ranging from 1.5° to 21.5°; two trim runs where C_T/σ = 0.14 and C_T/σ = 0.15 were also conducted. The temperature range encompassed 17.72 – 22.11 °C.

TRT consisted only of single rotor runs with collective sweeps ranging from 0° to 20°. The chamber temperature ranged from 20.11 – 21.15 °C.

DATA PROCESSING

Software running on the MATLAB R2023a programming platform was used to process the data for EDM-1 and TRT performance data (Ref. 4). Data processing steps are shown in Fig. 7. First, the raw force and torque data were transformed to account for FTS location and weight tares. Weight tares were performed by subtracting the mean of the first 2 seconds of FTS data from the subsequent FTS data in each run; the rotors were not spinning during the first 2 seconds. Then a 4th order 2 Hz low pass Butterworth zero-phase digital filter was applied to attenuate the high frequency components and preserve the low frequency components. An example of filtered and unfiltered coefficient of thrust data over time from EDM-1 is shown in Fig. 8 to highlight the need for filtering.

Additionally, an estimated mechanical power fitted curve for the upper and lower rotor must be created for each RPM tested in the EDM-1 runs. The FTS measures the moments of the aircraft; the net yaw moment is nearly zero for the coaxial configuration, thus, the electrical power must be used to get the rotor shaft's mechanical power. Since each rotor has its own motor, by running only one rotor, the motor efficiency can be calibrated as the FTS is measuring the torque of that single rotor. Since the other rotor is still present even if it's not spinning, its presence affects the flow and air loads, so performance of the rotating rotor is not meaningful; the primary purpose of the single rotor EDM-1 test is to simply estimate motor efficiency.

For example, in EDM-1: Test 1, an estimated mechanical power fitted curve was created for the upper rotor using runs 22 and 24 (upper rotor only runs). Then, an estimated mechanical power fitted curve was created for the lower rotor using runs 21 and 23 (lower rotor only runs). EDM-1 motor efficiency versus electrical power for upper and lower rotor single rotor configurations for various Reynolds numbers is shown in Fig. 9. From the motor efficiency curves, the estimated shaft power can be calculated. With the estimated power, the figure of merit and coefficient of power can be calculated as well.

Test data was acquired using several systems that had different time clocks. To synchronize the data, a global time clock with a frequency of 2000 Hz was defined based

on the maximum start and minimum end time of each parameter time clock. Each run started with a 5-degree collective followed by a rapid collective stepdown prior to the main data collection period, which produced a readily identifiable signal in the FTS, power, and collective input data for time syncing via slope identification realignment.

All FTS (3 forces, 3 torques), helicopter control (RPM and collective), and power system data (current) for each run was interpolated to the global time clock to ensure all data records had the same length and occurred at the same time. Furthermore, interpolation allows for calculating the FM over time, which requires C_T and C_P to be the same vector length.

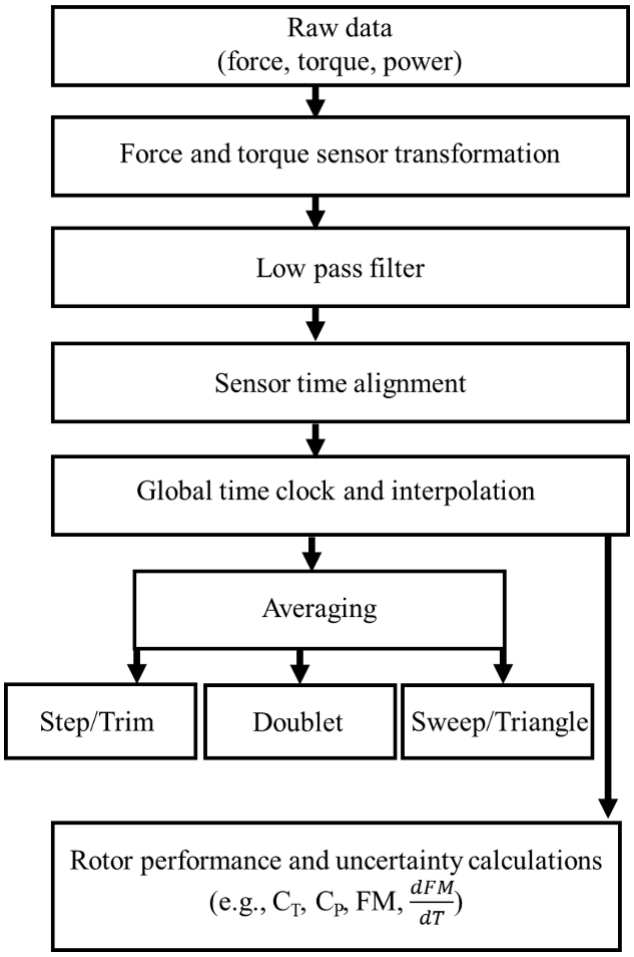

Figure 7. Data processing flow chart.

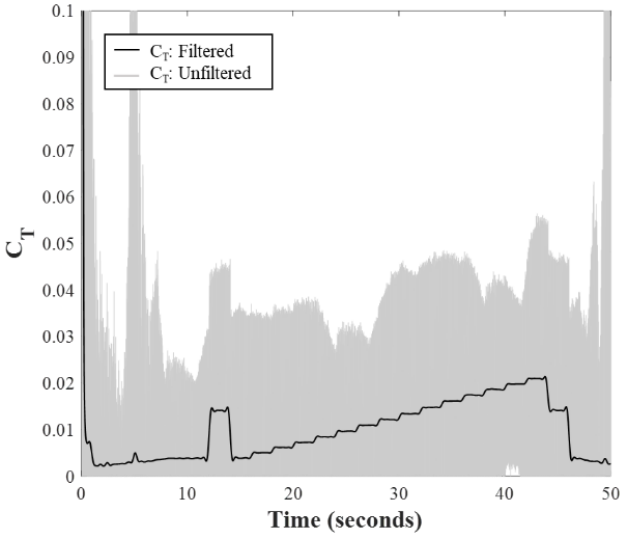

Figure 8. Coefficient of thrust filtered and unfiltered example run from EDM-1 (RPM = 2,200 ρ = 0.010 kg/m^3).

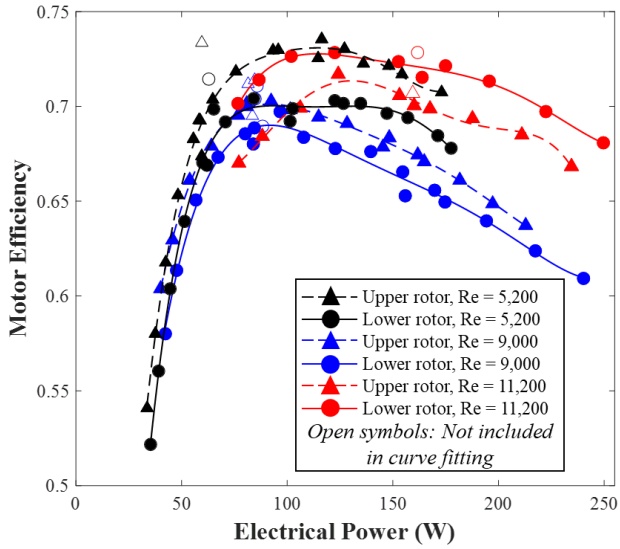

Figure 9. EDM-1 motor efficiency versus electrical power for upper and lower rotor single rotor configurations.

Processing types

Due to the types of runs performed, the data was split into processing types: step/trim, doublet, and sweep/triangle.

For data sets identified as a step type, the collective input was searched to identify positive and negative slopes to locate dwells. The center of each dwell (or lull) is then identified, and the data is averaged for approximately 29 revolutions one second before the end of the dwell. This

method of averaging was used due to the unsteady data immediate after a collective change. Averaging the data one second before the end of a dwell allows time for the air flow to steady out. Fig. 10 shows C_T and upper rotor collective over time with the start and end of dwell identified, as well as the data range that was averaged. The same process was performed for all trim runs, though averaged data is not presented in performance results due to unsteadiness of control settings as shown in Fig. 11.

For doublet runs the slope of the upper and/or lower cyclic time history was searched, and each dwell was identified. The center of each dwell was located, and the data averaged for approximately 29 revolutions one second prior to the end of the dwell. This process is similar to the step data processing technique, except instead of collective slope search a cyclic slope search is performed. Figure 12 shows a doublet example for EDM1 for both rotors at a condition of RPM = 2,200 ρ = 0.010 kg/m^3, upper rotor cyclic doublets at $C_T/\sigma = 0.135$.

For sweep and triangle runs, the stop and start are identified based on collective dynamics, and every 200th point was selected, see Fig. 13. Selecting every 200th point reduces the amount of data, therefore speeding up processing time. However, the complete data set is available if needed. Data from the sweep cases are not averaged over time due to constant change in control input.

Finally, with the data processed and averaged (step/trim and doublet only), performance variables such as figure of merit (FM) and power can be calculated.

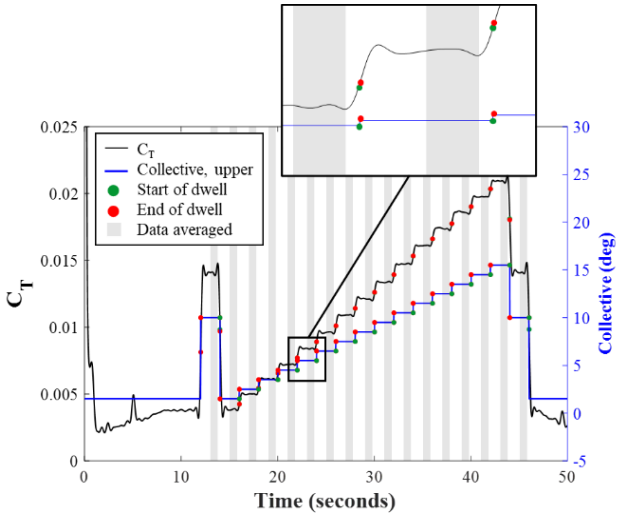

Figure 10: Data processing step example from EDM-1 for both rotors (RPM = 2,200 ρ = 0.010 kg/m^3).

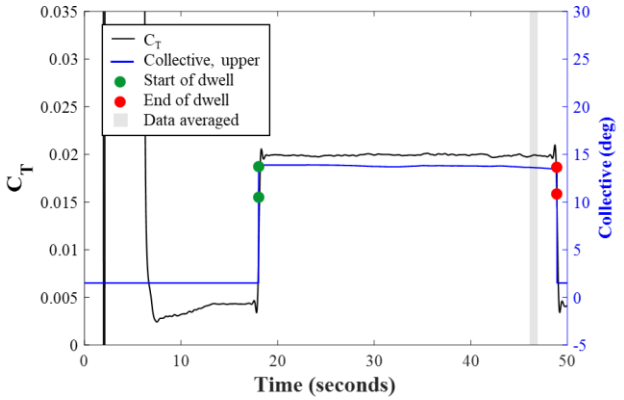

Figure 11. Data processing trim example from EDM-1 for both rotors (RPM = 2,043 ρ = 0.018 kg/m^3).

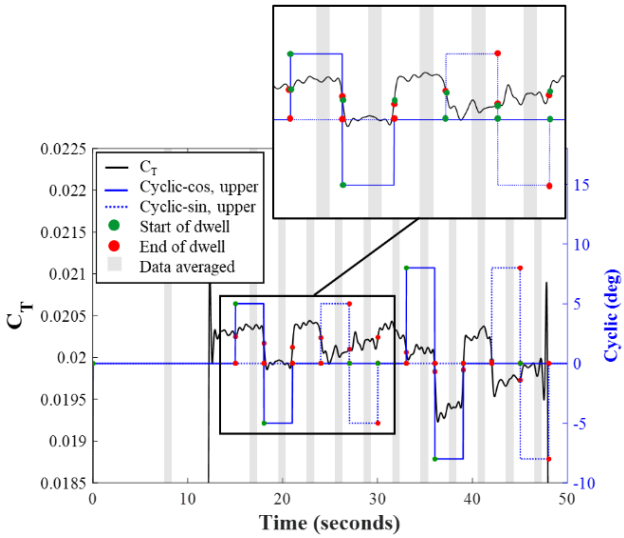

Figure 12. Data processing doublet example from EDM-1 for both rotors (RPM = 2,200 ρ = 0.010 kg/m^3, upper rotor cyclic doublets at $C_T/\sigma = 0.135$.

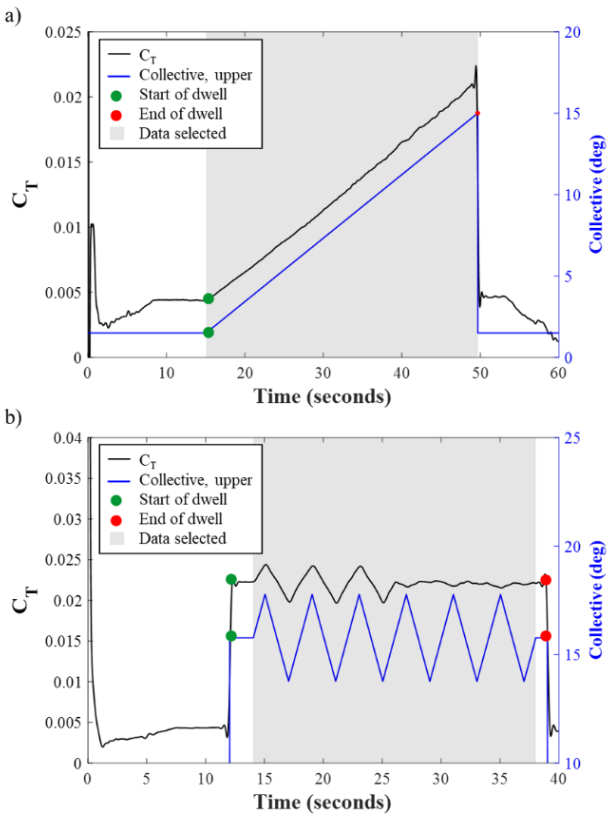

Figure 13. Data processing a) sweep and b) triangle example for EDM-1 for both rotors at RPM = 2,200, ρ = 0.014 kg/m^3 collective sweep and RPM = 2,043, ρ = 0.0185 kg/m^3 collective ramps, respectively.

RESULTS

Performance results from EMD-1 with and without the cruciform box, and TRT are presented for all step runs. For the coaxial runs, the presented torque and power is the summation of both rotors. The FM and coefficients are based on the disk area of one rotor, as appropriate for coaxial rotorcraft (Ref. 5). The blade loading (C_T/σ) is based on the total torque and total blade area of both rotors.

To compare the data, the parameters of C_T, C_P, C_T/σ and figure of merit are used. Figure of merit is used to gauge the efficiency of a rotor and is defined as the ratio between the ideal and actual power of the rotor. Figure of merit values presented for coaxial EDM-1 were calculated using estimated power from the motor efficiency (mechanical power). TRT and EDM-1 single rotor figure of merit calculations used power from the measured rotor torque.

EDM1 Experimental Results

Performance results from EDM-1 for various Reynolds number without the cruciform box are shown in Fig. 14 for a) C_P versus C_T and for b) FM vs blade loading for a range of Reynolds numbers. A Reynolds number range from 5,200 to 14,500, with RPM variations (2,043 – 2,550) and density variations (0.01 and 0.03 kg/m^3) are shown.

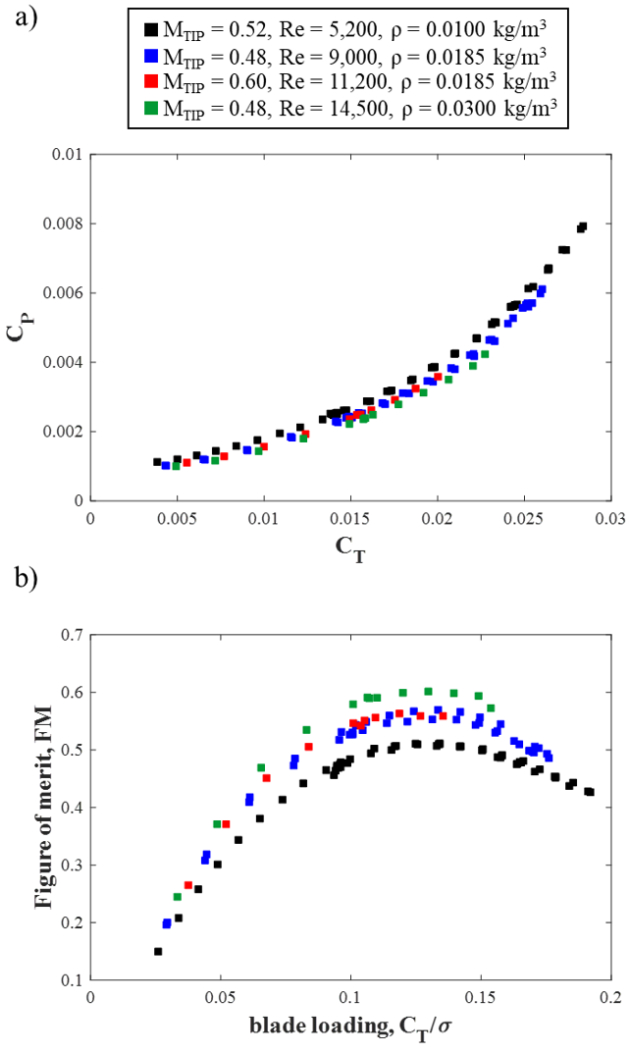

Figure 14. a) Coefficient of thrust versus Coefficient of power and b) figure of merit versus blade loading for EDM1-1 for coaxial rotor configuration without cruciform box.

Performance results from EDM-1 for various Reynolds number with the cruciform box are shown in Fig. 15 for a) C_P versus C_T and for b) FM vs blade loading for a range of Reynolds numbers. A Reynolds number range from 5,200 to 14,500, with RPM variations (2043 - 2550) and density variations (0.01 and 0.03 kg/m^3) are shown.

The lower the Reynolds number, the higher the C_P was for a given C_T for all conditions. This is further revealed in the FM. A maximum FM is seen at a blade loading (C_T/σ) between 0.12 and 0.14, and an increase in FM with increasing Reynolds number due to the increased density or RPM. The presence of the cruciform box resulted in a higher peak FM compared to without the cruciform box, which is due in part to the cruciform box acting like a ground plane.

Results from EDM-1 with and without the cruciform box did not reveal an abrupt drop in FM as blade loading was increased for all Reynolds numbers presented.

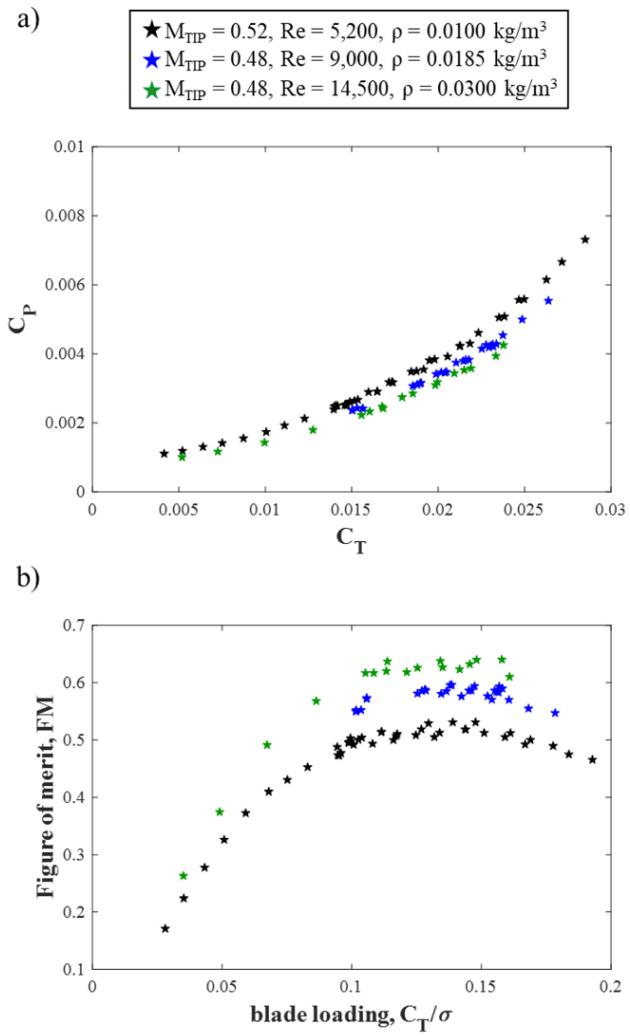

Figure 15. a) Coefficient of thrust versus Coefficient of power and b) figure of merit versus blade loading for EDM1-1 for coaxial rotor configuration with cruciform box.

TRT Experimental Results

Experimental performance results for TRT are shown in Fig. 16 for a) C_P versus C_T and for b) FM vs blade loading for a tip Mach number from 0.65 to 0.85. As M_{tip} increases, the C_P decreases for a given C_T. A peak FM of 0.48 is observed at an M_{tip} of 0.7 with a blade loading of 0.13; the drop in FM when blade loading is increased beyond 0.13 indicates the onset of blade stall. The TRT test concluded an advancing tip Mach of 0.85 (hover tip Mach of 0.77) is the limit before reaching drag divergence for Ingenuity rotors.

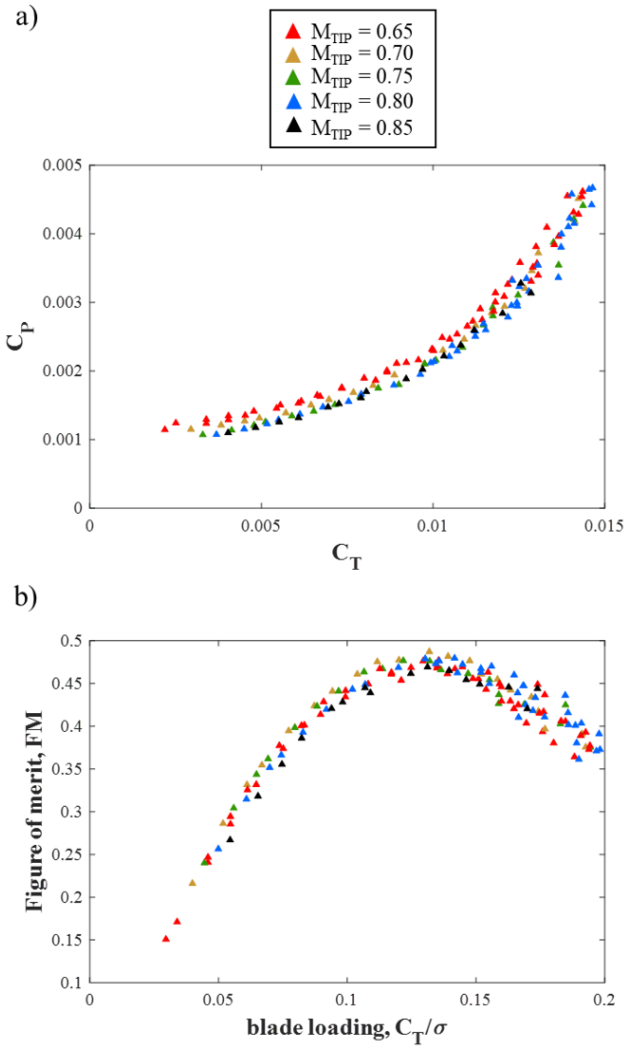

Figure 16. a) Coefficient of thrust versus Coefficient of power and b) figure of merit versus blade loading for TRT.

Data Quality

A data quality analysis was performed for the EDM-1 coaxial rotor configuration with and without cruciform box and TRT using the method of propagation of uncertainty. An uncertainty propagation analysis was performed to study the error in key performance parameters resulting from error in multiple measured variables (Ref. 6). For example, for figure of merit from the EDM-1 test propagation variables include taking the partial derivative of thrust (T), omega (Ω), electrical power ($P_{electric}$), and standard deviation of these variables ($\bar{\sigma}$). Furthermore, since electric power is determined from a fitted curve (see Fig. 9) that error also must be accounted for ($\bar{\sigma}_{Fit}$). The same process is performed for blade loading, thrust, and omega. Uncertainty due to instrumentation is not independently accounted for at this time. The uncertainly propagation of error for figure of merit from the EDM-1 test can be calculated using equation 1.

Equation. 1

$$FM = FM \pm 2\sqrt{\left(\frac{dFM}{dT}\bar{\sigma}_T\right)^2 + \left(\frac{dFM}{d\Omega}\bar{\sigma}_\Omega\right)^2 + \left(\frac{dFM}{dP_{Electric}}\bar{\sigma}_{P,electric}\right)^2 + \left(\frac{dFM}{dP_{Electric}}\bar{\sigma}_{Fit}\right)^2}$$

Figure of merit versus blade loading for EDM-1 without and with cruciform box with uncertainty analysis performed is shown in Figs. 17 and 18, respectively. Uncertainty is shown by use of error bars in the x and y direction to account for uncertainty for figure of merit and blade loading, respectively. In general, as a peak figure of merit is reached an overall increase in uncertainty for all Reynolds numbers is present. The presence of the cruciform box (Fig. 18) revealed a larger uncertainly when compared to without the cruciform box (Fig. 17), which may be due to the turbulent wake interference of the cruciform box.

Figure of merit versus blade loading for TRT with uncertainty analysis performed is shown in Fig. 19. Similar to EDM-1, as blade loading increases so does uncertainty. In general, uncertainty is lower for the EDM-1 runs because the increased complexity from the second rotor adds additional unsteadiness to the measurement.

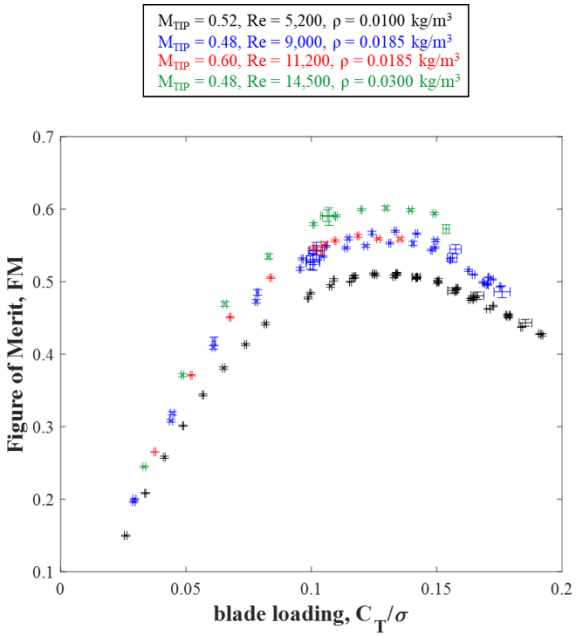

Figure 17. Figure of merit versus blade loading for EDM-1 coaxial configuration with uncertainty analysis performed without cruciform box.

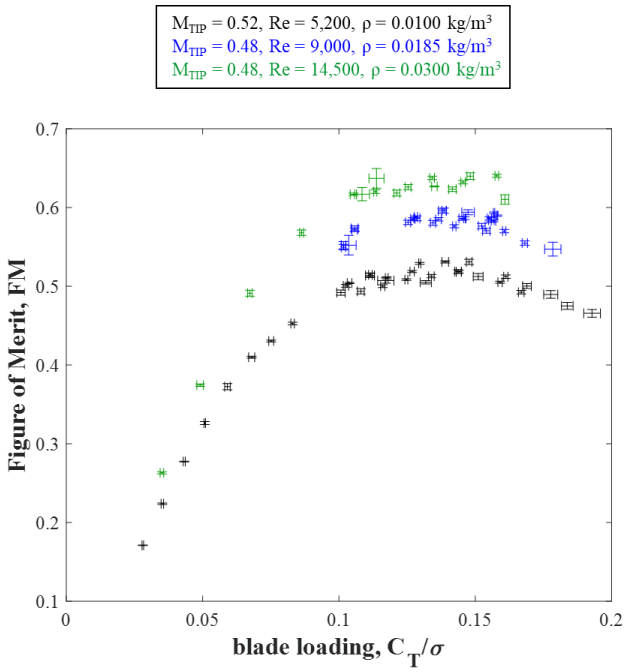

Figure 18. Figure of merit versus blade loading for EDM-1 coaxial configuration with uncertainty analysis performed with cruciform box.

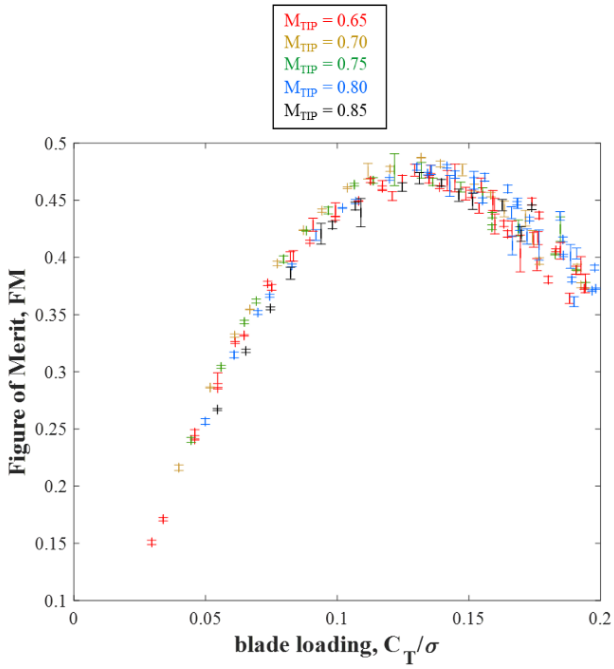

Figure 19. Figure of merit versus blade loading for TRT with uncertainty analysis performed.

CONCLUSIONS

Performance results from the (EDM-1) with and without a cruciform box and the TRT at the JPL in the 25-foot Space Simulator were presented. The experimental setup, test matrix, data processing, and performance results for EDM-1 and TRT campaigns were discussed for each of these tests.

The TRT was performed to understand the performance behavior of a single rotor using the Mars helicopter (Ingenuity) blade geometry at high Mach tip speeds between 0.65 and 0.85. Results from TRT indicated a reduced hovering rotor efficiency for a tip Mach number greater than 0.75. The peak was observed with figure of merit of 0.48 at a tip Mach number of 0.7 with a blade loading of 0.13. Higher blade loadings result in lower FM due to the onset of stall.

EDM-1 was tested for a range of Reynolds numbers between 5,200 to 14,500 with a range of densities and RPM's, where a maximum FM was seen at a blade loading between 0.12 and 0.14.

In summary, the results from the EDM-1 test campaign showed that stall occurred as a soft limit—meaning there is no abrupt cliff-like drop in FM with increased blade loading. The TRT test sought to identify signs of drag divergence and concluded the Ingenuity rotors can safely reach advancing tip Mach of 0.85 (hover tip Mach of 0.77).

ACKNOWLEDGEMENTS

Authors would like to acknowledge the entire Mars Sample Return program team for all their support. Special thanks to Wayne Johnson and Larry Meyn for their mentorship. Thank you to Meridith Segall for providing artistic advice.

The authors acknowledge the Mars Sample Return Project, NASA's Jet Propulsion Laboratory, NASA Ames Research Center, NASA Langley Research Center, AeroVironment, and the NASA Convergent Aeronautics Solutions (CAS) Project for funding and support.

This research was carried out at the Jet Propulsion Laboratory, California Institute of Technology, under a contract with the National Aeronautics and Space Administration.

The decision to implement Mars Sample Return will not be finalized until NASA's completion of the National Environmental Policy Act (NEPA) process. This document is being made available for information purposes only.

REFERENCES

1. Mars Exploration Program and the Jet Propulsion Laboratory, "Mars Helicopter Flight Log," NASA, dated April 26, 2023, https://mars.nasa.gov/technology/helicopter (accessed July 14, 2023).
2. Withrow-Maser, Shannah, Cummings, H., Johnson, W., Malpica, C., Meyn, L., Schatzman, N., Young, L., Keennon, M., Pipenberg, P., Grip, H., Tzanetos, T., Allan, B., Chan, A., Koning, W., and Ruan, A., "Mars Sample Recovery Helicopter: Rotorcraft to Retrieve the First Samples from the Martian Surface", Presented at the Vertical Flight Society's 79th Annual Forum & Technology Display, West Palm Beach, FL, May 16–18, 2023.
3. Harrell, J. W., and Argoud, M. J., "The 25-ft Space Simulator at the Jet Propulsion Laboratory," NASA CR 106222, Oct. 1969.
4. MATLAB, version 9.14.0.2206163 (R2023a), The MathWorks Inc., Natick, Massachusetts, 2010.
5. Johnson, W., Rotorcraft Aeromechanics. New York: Cambridge University Press, 2013.
6. Taylor, B. N. and Kuyatt, C. E., "Guidelines for Evaluating and Expressing the Uncertainty of NIST Measurement Results, National Institute of Standards and Technology", NIST technical note 1297, September 1994.